



Cite this: *Polym. Chem.*, 2016, 7, 2492

# Development of a transition metal-free polymerization route to functional conjugated polydiynes from a haloalkyne-based organic reaction†

Yun Zhang,<sup>a,b</sup> Engui Zhao,<sup>a,b</sup> Haiqin Deng,<sup>a,b</sup> Jacky W. Y. Lam<sup>\*a,b</sup> and Ben Zhong Tang<sup>\*a,b,c,d</sup>

The development of an efficient transition metal-free polymerization route has been an active research topic in polymer science owing to its low synthetic cost and decreased metal residue and hence elevated material performance in the products. In this work, we report a new such method for constructing conjugated polydiynes based on the organic reaction of 1-haloalkyne. In the presence of potassium iodide, the polymerizations of 1,2-bis[4-(iodoethynyl)phenyl]-1,2-diphenylethene (**1**), 1,4-bis(2-iodoethynyl)benzene (**2**) and 4,4'-bis(2-iodoethynyl)-1,1'-biphenyl (**3**) proceed smoothly in *N,N*-dimethylformamide at 120 °C under nitrogen, producing **P1–3** consisting of alternate aromatic and 1,3-diyne moieties in moderate to satisfactory yields. While **P1** possesses good solubility in common organic solvents, **P2** and **P3** are insoluble due to their rigid structures. All the polymers are thermally stable, losing 5% of their weight at a high temperature of up to 352 °C. A homogeneous film of **P1** can be readily obtained by spin-coating its solution, which shows high and UV-tunable refractive index ( $n = 2.1125\text{--}1.7747$ ) in a wide wavelength range (400–900 nm). A well-defined fluorescent photopattern can be generated by UV irradiation of the polymer film through a copper mask. This work thus opens a new avenue for constructing conjugated polymers with advanced functionalities.

Received 11th January 2016,  
Accepted 2nd March 2016

DOI: 10.1039/c6py00050a

www.rsc.org/polymers

## Introduction

Synthetic polymeric materials are gaining increasing attention due to their superior properties, such as high mechanical strength, good thermal stability and excellent macroscopic processability, and hence potential high-tech applications. The development of facile and efficient methodologies towards various polymers is thus a long-standing research topic and the goal of both scientists and engineers. Currently, most of

the polymerizations are derived from the organic reactions of small molecules. For an ideal organic reaction to be developed into a new polymerization method, several criteria should be satisfied, which include but are not limited to high reaction efficiency and conversion rate, wide monomer scope and high regio-/stereoselectivity. In this way, the derived polymerization reaction can afford polymers in good yields with high molecular weights and specific structures. Furthermore, to ensure the polymers obtained are practically useful, sensible monomer design is necessary, which is closely related to the properties of the polymers obtained.

Triple bond reactions constitute a considerable portion of the organic reactions and C≡C serves as a versatile building block in the construction of various functional structures. In many triple-bond reactions, such as cyclotrimerization, addition and metathesis, the triple bonds are transformed to aromatic rings or double bonds, affording conjugated products with novel electronic and optical properties. Therefore, triple-bond-derived polymerization reactions are powerful methods for the preparation of conjugated polymers.<sup>1–11</sup> Our research group is interested in constructing functional conjugated macromolecules from alkyne monomers.<sup>12–17</sup> We have prepared hyperbranched polyarylenes with unique optical and

<sup>a</sup>HKUST-Shenzhen Research Institute, No. 9 Yuexing 1st RD, South Area, Hi-tech Park, Nanshan, Shenzhen 518057, China. E-mail: chjacky@ust.hk, tangbenz@ust.hk

<sup>b</sup>Department of Chemistry, Division of Life Science, State Key Laboratory of Molecular Neuroscience, Institute for Advanced Study, Institute of Molecular Functional Materials, Division of Biomedical Engineering, The Hong Kong University of Science and Technology, Clear Water Bay, Kowloon, Hong Kong, China

<sup>c</sup>Guangdong Innovative Research Team, SCUT-HKUST Joint Research Laboratory, State Key Laboratory of Luminescent Materials and Devices, South China University of Technology, Guangzhou 510640, China

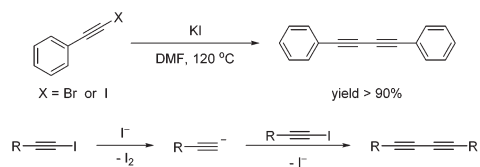
<sup>d</sup>Hong Kong Branch of Chinese National Engineering Research Center for Tissue Restoration and Reconstruction, China

† Electronic supplementary information (ESI) available: Crystal data for model compound **7**. CCDC 1423561. For ESI and crystallographic data in CIF or other electronic format see DOI: 10.1039/c6py00050a

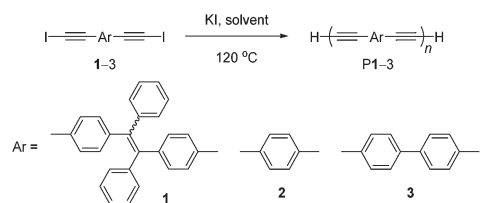
photophysical properties by the polycyclotrimerization of diynes  $R-(C\equiv CH)_2$  catalyzed by tantalum or cobalt complexes.<sup>18–22</sup> As an extension of this system, we have developed a polymerization route to construct nitrogen-rich hyperbranched polytriazines by polycyclotrimerization of dinitriles  $R-(C\equiv N)_2$ .<sup>23</sup> Besides, we also utilized alkyne–azide cycloaddition to construct functional polytriazoles with heteroatom-containing backbones.<sup>15,24</sup> Specifically, we successfully developed various click polymerization systems conducted in the absence or presence of a metal or non-metal catalyst.<sup>24–30</sup> Additionally, we embarked on the development of thiol–yne click polymerization based on alkyne hydrothiolation for the synthesis of sulfur-containing unsaturated polymers.<sup>31</sup> Due to the high efficiency of the thiol–yne addition reaction, functional poly(vinylene sulfide)s can be readily obtained *via* rhodium-catalyzed, secondary amine-mediated and catalyst-free thiol–yne click polymerizations.<sup>32–34</sup>

In the above examples, the triple bonds open and new double bonds form during the polymerization process. We also work on other polymerization reactions, in which the triple bonds of the monomers remain intact after the polymerization. The preservation of  $C\equiv C$  results in conjugated structures and endows the polymeric products with potential thermal, electronic and optical properties.<sup>35,36</sup> For example, luminescent poly(arylene ethynylene)s with tetraphenylethene (TPE) and silole moieties were prepared by palladium-catalyzed Sonogashira polycoupling of terminal alkynes and aryl halides.<sup>37</sup> Compared with those containing ethynylene units, polymers with 1,3-diyne functionalities demonstrate a better performance as semiconductors, optical materials and molecular recognition systems.<sup>2,38,39</sup> Generally, diyne-containing polymers can be readily obtained by the homo-polycoupling reactions of diyne monomers catalyzed by transition metal catalysts, such as copper and palladium. For example, under Glaser–Hay oxidative coupling conditions and in the presence of  $CuCl$ , soluble linear and hyperbranched polydiynes were produced in almost quantitative yields with high molecular weights.<sup>40–43</sup> These two tools have been widely used to produce triple bond-containing polymers but they show some disadvantages. While the Sonogashira polycoupling reaction requires a strict stoichiometric balance between monomers in order to generate a high molecular weight polymer, the copper residue in the polymers generated by Glaser–Hay homo-polycoupling may deteriorate their material properties.

Haloalkynes exhibit both controllable electrophilic and nucleophilic properties. Because of such functionality, they have emerged as powerful and versatile synthons in synthetic organic chemistry.<sup>44</sup> In 2010, Jiang and co-workers discovered a transition metal-free homocoupling reaction to synthesize symmetrical 1,3-diynes from 1-haloalkynes (Scheme 1).<sup>45</sup> This reaction is mediated by potassium iodide without employing any transition metal, base or oxidant, and is different from previous protocols, which use terminal alkynes as reactants and transition-metal complexes or reactive alkynylmagnesium compounds as catalysts. Taking advantage of the inexpensive additive used, simple procedure and high product yield, we



**Scheme 1** Transition metal-free homocoupling of 1-haloalkyne and its plausible mechanism.



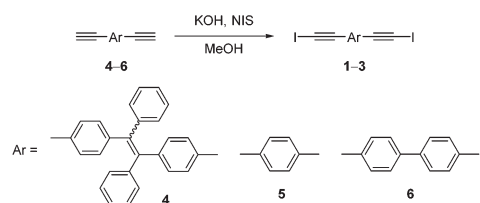
**Scheme 2** Construction of conjugated polydiynes by KI-mediated transition metal-free homo-polycoupling of bis(iodoalkynes).

intend to develop the KI-mediated coupling reaction of 1-haloalkyne into a novel polymerization route in this work. In this regard, bis(iodoalkyne)s **1–3** were prepared and used as monomers for constructing polymers. All the monomers can be polymerized in the presence of KI, generating **P1–3** in moderate to satisfactory yield in a short time (Scheme 2). While **P1** readily dissolves in common organic solvents, **P2** and **P3** are insoluble. We herein report the synthesis of the polymers and present the material properties of **P1** in this work.

## Results and discussion

### Monomer design

The first step in developing a polymerization reaction from a small molecular reaction is the design and synthesis of monomers bearing two reactive functional groups. We thus prepared 1,2-bis[4-(iodoethynyl)phenyl]-1,2-diphenylethene (**1**) by the reaction of 1,2-bis(4-ethynylphenyl)-1,2-diphenylethene (**4**) with *N*-iodosuccinimide in an alkaline medium (Scheme 3).<sup>46,47</sup> We also synthesized 1,4-bis(2-iodoethynyl)benzene (**2**) and 4,4'-bis(2-iodoethynyl)-1,1'-biphenyl (**3**) by the same reaction route, using 1,4-diethynylbenzene (**5**) and 4,4'-diethynylbiphenyl (**6**) as starting materials.<sup>48</sup> All the monomers were obtained in high yields. Their structures were characterized



**Scheme 3** Synthetic route to monomers **1–3**.

by standard spectroscopy methods with satisfactory results. Details can be found in the Experimental section.

### Polymerization

We first used monomer **1** to optimize the conditions for the polymerization. We initially investigated the solvent effect on the polymerization. According to the small molecular reaction, it is better to conduct the polymerization at high temperature. Various solvents with a high boiling point and different solvating powers and polarities were thus tested. Among all the tested solvents, *N,N*-dimethylformamide (DMF) was the most appropriate one for polymerization, yielding a soluble polymer with the highest molecular weight ( $M_w = 18\,700$ ) in a higher yield (69%). A satisfactory yield (53%) was also obtained when the polymerization was conducted in dimethylsulfoxide (DMSO), but the molecular weight of the product became lower ( $M_w = 7100$ ). The polymerizations in non-polar solvents, such as 1,4-dioxane and *o*-xylene, however, generated oligomers in poor yields, indicating that they were not suitable for polymerization.

We then followed the time course of the polymerization by calculating the isolation yield of the polymer obtained and measuring its molecular weight by GPC analysis. As shown in Table 2, within the first 6 h, the yield increases from 13% to 72% and the molecular weight of the polymer also increases from 2900 to 20 100. Further prolonging the reaction time to 24 h, however, leads to no further increase in the isolation yield and molecular weight. Instead, some insoluble gel-like substances were formed when the reaction time exceeds 6 h (Table 2, no. 4 and no. 5), which lowered the overall yield and the polymer's molecular weight. The time course study

suggests that 6 h is the most suitable time for the polymerization (Table 2, no. 3).

According to the mechanism shown in Scheme 1, KI plays an important role in the polymerization and serves as an additive to remove the iodine cation from the monomer. Therefore, we studied the effect of its amount on the polymerization (Table 3). At a KI concentration two times higher than that of **1**, a polymer with the highest molecular weight ( $M_w = 20\,100$ ) was obtained in a satisfactory yield (72%, Table 3, no. 2). By further increasing the KI amount, the molecular weight of the polymeric product drops dramatically but the isolated yield remains pretty high. On the other hand, reducing the amount of KI to a value equal to the monomer concentration decreases both the yield and molecular weight. Therefore, the ratio of KI and monomer **1** was kept at 2 : 1 in the following experiments.

We then investigated the influence of monomer concentration on the polymerization reaction. Generally speaking, a higher monomer concentration will facilitate intermolecular collision between monomers, leading to a better polymerization result. As shown in Table 4, when the monomer concentration was increased from 0.05 M to 0.20 M, the isolation yield was enhanced from 47% to 91% accordingly. The dependence of molecular weight on the monomer concentration, however, was different. Increasing the monomer concentration from 0.10 M to 0.20 M results in partial gelation, yielding a partially soluble polymer with a molecular weight of merely 10 700. These results demonstrate that the present polymerization is efficient and does not require the use of reacting monomers at high concentration.

Many polymerization reactions are sensitive to oxygen, especially those involving radical species. To check the sensi-

**Table 1** Solvent effect on the polymerization<sup>a</sup>

No.	Solvent	Yield (%)	$M_w^b$	$M_w/M_n^b$
1	DMF	69	18 700	2.3
2	DMSO	53	7100	1.6
3	1,4-Dioxane	26	2800	1.3
4	<i>o</i> -Xylene	18	3400	1.3

<sup>a</sup> Carried out in different solvents using **1** as the monomer under nitrogen in the presence of KI at 120 °C for 24 h.  $[1] = 0.1$  M.  $[KI]/[1] = 2$ . <sup>b</sup> Determined by GPC in THF on the basis of a linear polystyrene calibration.

**Table 2** Time course of the polymerization<sup>a</sup>

No.	Time (h)	Yield (%)	$M_w^b$	$M_w/M_n^b$
1	1	13	2900	1.2
2	3	55	7100	1.5
3	6	72	20 100	2.4
4	12	63	16 800	1.8
5 <sup>c</sup>	24	69	18 700	2.3

<sup>a</sup> Carried out in DMF using **1** as the monomer under nitrogen in the presence of KI at 120 °C.  $[1] = 0.1$  M.  $[KI]/[1] = 2$ . <sup>b</sup> Determined by GPC in THF on the basis of a linear polystyrene calibration. <sup>c</sup> Data taken from Table 1, no. 1.

**Table 3** Effect of additive on the polymerization<sup>a</sup>

No.	$[KI]/[1]$	Yield (%)	$M_w^b$	$M_w/M_n^b$
1	1	52	6700	1.4
2 <sup>c</sup>	2	72	20 100	2.4
3	3	77	11 600	2.0
4	4	75	8600	1.6

<sup>a</sup> Carried out in DMF using **1** as the monomer under nitrogen in the presence of KI at 120 °C for 6 h.  $[1] = 0.1$  M. <sup>b</sup> Determined by GPC in THF on the basis of a linear polystyrene calibration. <sup>c</sup> Data taken from Table 2, no. 3.

**Table 4** Effect of monomer concentration on the polymerization<sup>a</sup>

No.	$[1]$	Yield (%)	$M_w^b$	$M_w/M_n^b$
1	0.05	47	5000	1.3
2 <sup>c</sup>	0.10	72	20 100	2.4
3	0.15	79	10 300 <sup>d</sup>	1.6
4	0.20	91	10 700 <sup>d</sup>	1.9

<sup>a</sup> Carried out in DMF using **1** as the monomer under nitrogen in the presence of KI at 120 °C for 6 h.  $[KI]/[1] = 2$ . <sup>b</sup> Determined by GPC in THF on the basis of a linear polystyrene calibration. <sup>c</sup> Data taken from Table 2, no. 3. <sup>d</sup> Soluble fraction.

**Table 5** Effect of air on the polymerization<sup>a</sup>

No.	Yield (%)	$M_w^b$	$M_w/M_n^b$
1 <sup>c</sup>	72	20 100	2.4
2 <sup>d</sup>	42	4600	1.3

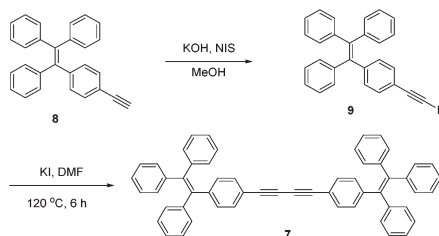
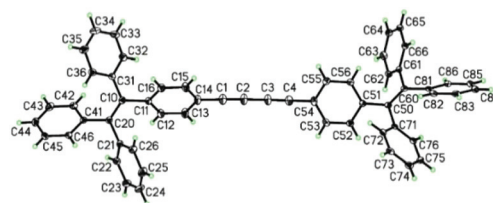
<sup>a</sup> Carried out in DMF using **1** as the monomer in a Schlenk tube in the presence of KI at 120 °C for 6 h. [**1**] = 0.1 M, [KI]/[**1**] = 2. <sup>b</sup> Determined by GPC in THF on the basis of a linear polystyrene calibration. <sup>c</sup> Under a nitrogen flow. Data taken from Table 2, no. 3. <sup>d</sup> In open air.

tivity of the present polymerization to air, we compared the polymerization results obtained under nitrogen and in open air (Table 5). The polymerization conducted in open air gives a poorer result than that obtained under nitrogen, presumably due to the high sensitivity of the iodine radical involved in the reaction mechanism to oxygen. Clearly, the nitrogen environment is essential for efficient polymerization.

To sum up, it is better to carry out the homo-polycoupling of **1** in DMF under nitrogen at a monomer concentration of around 0.10 M and KI/1 ratio of 2. Thus, we used the same conditions for polymerizing **2** and **3**. While both monomers can be polymerized in moderate yields, the polymers obtained are insoluble. The rod-like, aromatic structures of the monomers may impact their resulting polymers with tight molecular packing and rigid conformation, thus dramatically lowering their processability. On the other hand, P1 may show weak interactions and large free volumes between the polymer chains due to the twisted conformation of the TPE unit of **1**. This may explain why it can dissolve readily in common organic solvents, such as THF, dichloromethane, chloroform, *etc.*

### Model reaction

In order to confirm the occurrence of the homo-polycoupling reaction and gain insight into the structure of the polymer, a model compound **7** was synthesized (Scheme 4). Compound **9** was prepared by iodination of 1-(4-ethynylphenyl)-1,2,2-triphenylethene (**8**) using NIS in methanol. Its homo-coupling was carried out under conditions similar to those for preparing the polymers. The model compound **7** generated was purified by silica gel column chromatography using a hexane/DCM mixture as an eluent. Single crystals of **7** were obtained from its chloroform/hexane solution and analyzed by X-ray crystallography. The results are shown in Fig. 1 and Table S1 in the ESI.† As shown in Fig. 1, the molecular structure clearly shows the linear 1,3-diyne

**Scheme 4** Synthetic route to model compound **7**.**Fig. 1** ORTEP drawing of the crystal structure of model compound **7**. (CCDC 1423561).

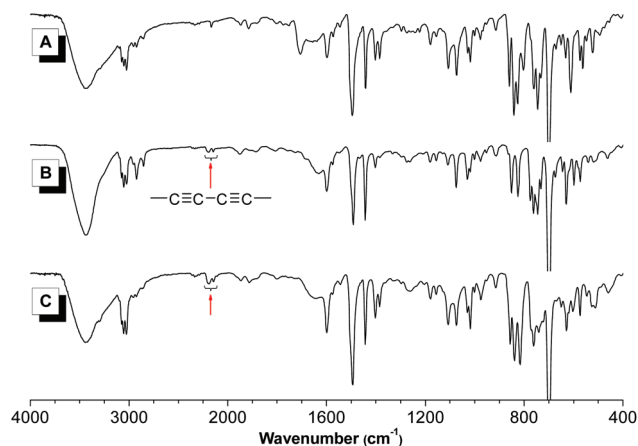
unit, thus verifying the success of the reaction. Comparison between **7** and the resulting polymer will give strong supportive information on the structural analysis of the latter.

### Structure characterization

Monomer **1**, model compound **7** and polymer P1 were characterized by standard spectroscopic techniques, such as FT-IR, <sup>1</sup>H NMR and <sup>13</sup>C NMR spectroscopy, from which satisfactory analysis data corresponding to their molecular structures were obtained. The featured peaks of P1 in each spectrum are discussed in detail in the following text.

The IR spectrum of P1 is shown in Fig. 2C. For comparison, the spectra of monomer **1** and model compound **7** are also given in the same figure (Fig. 2A and B, respectively). The absorption peaks associated with the C≡C–C≡C stretching in model compound **7** are observed at 2199 and 2147 cm<sup>-1</sup>, respectively. These two absorption peaks are also observed in the IR spectrum of the polymer, but are absent in monomer **1**. This confirms the success in the formation of the 1,3-diyne structure in the polymer backbone and the occurrence of the homo-polycoupling reaction. Other peaks in the monomer are well preserved in the polymer.

Fig. 3 shows the <sup>1</sup>H NMR spectra of **1**, **7** and P1 in deuterated DCM. Though all the protons resonate in the aromatic area, the peaks are well resolved and can be assigned due to their different chemical environments. As shown in Fig. 3, the peaks associated with the resonance of “a” protons are shifted

**Fig. 2** IR spectra of (A) **1**, (B) **7** and (C) P1 (Table 1, no. 1).

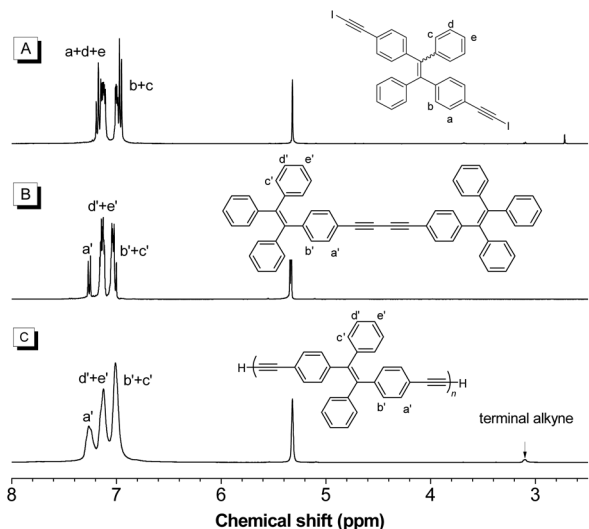


Fig. 3  $^1\text{H}$  NMR spectra of (A) **1**, (B) **7** and (C) **P1** (Table 1, no. 1) in dichloromethane- $d_2$ .

from  $\sim 7.27$  ppm in monomer **1** to  $\sim 7.70$  ppm ( $a'$  proton) in **7** and **P1** due to the formation of a new  $\text{C}\equiv\text{C}-\text{C}\equiv\text{C}$  unit after the polymerization (Table 1, no. 1). Compared with **7**, the peaks in **P1** are broader due to its polymeric nature. Interestingly, a small peak at  $\sim 3.0$  ppm is observed in **P1**, which suggests that the end groups are triple-bond functionalities. From the integral of this peak and those of the aromatic ones, the molecular weight of the polymer is calculated to be  $\sim 8270$ , which is consistent with the result ( $M_n = 8130$ ) by GPC analysis (Table 1, no. 1).

The structure of the resulting polymer is further verified by  $^{13}\text{C}$  NMR spectroscopy (Fig. 4). The peak representing the “a”

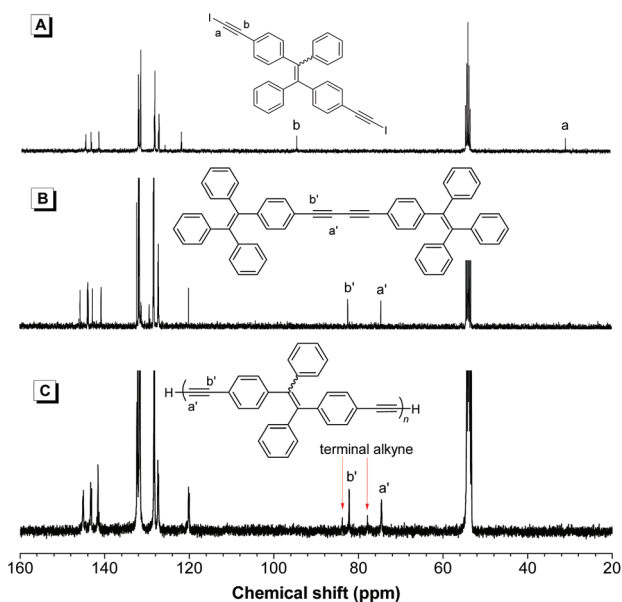


Fig. 4  $^{13}\text{C}$  NMR spectra of (A) **1**, (B) **7** and (C) **P1** (Table 1, no. 1) in dichloromethane- $d_2$ .

carbon of the triple bond experiences a large shift from 30.7 ppm in **1** to 74.5 ppm in **7** and **P1**. Meanwhile, the “b” carbon of the triple bond shifts to a higher field due to the formation of the 1,3-diyne unit (from 94.5 ppm to 82.4 ppm). The end groups of **P1** are also proven to be terminal alkynes, as suggested by the resonance peaks observed at 77.8 and 83.8 ppm. Other peaks corresponding to the resonances of the phenyl rings and the  $\text{C}=\text{C}$  double bond of the TPE unit inherited from the monomers are also observed. These results demonstrate the precise structure of the polymer and are well consistent with the results from the IR and  $^1\text{H}$  NMR analyses.

### Thermal stability

Thermogravimetric analysis (TGA) was employed to evaluate the thermal stability of the polymers. Thanks to its aromatic structure and 1,3-diyne unit, **P1** shows high thermal stability, losing merely 5% of its weight at a high temperature of 352  $^\circ\text{C}$  (Fig. 5). Moreover, **P1** retains 60% of its weight after being heated to 800  $^\circ\text{C}$ . The high mass preservation suggests the potential application of **P1** as a ceramic material. On the other hand, the relatively worse thermal stability of **P2** and **P3** might result from the low degree of polymerization and small  $M_w$  values, which might be attributed to the poor solubility of both monomers and polymers.

### Light refraction

Polymers with high refractive indices (RI or  $n$ ) are promising candidate materials for photonic applications. Particularly, polymers whose RI can be manipulated by light irradiation are useful in permanent data storage and holographic recording. **P1** shows good film-forming ability and can be fabricated into a tough thin film by spin coating its dichloroethane solution onto a silica substrate for RI measurement. As shown in Fig. 6, **P1** shows a high RI value of 2.1125–1.7747 in a wide wavelength range of 400–900 nm. The RI value at 632.8 nm is 1.8070, which is much higher than those of many commercial optical plastics at the same value. Such a high RI value may result from its high aromatic content and conjugation along the polymer backbone. Interestingly, **P1** is photosensitive.

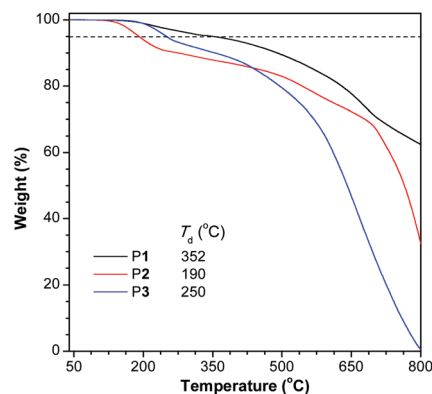


Fig. 5 TGA thermograms of **P1–3** recorded under nitrogen at a heating rate of 10  $^\circ\text{C min}^{-1}$ .

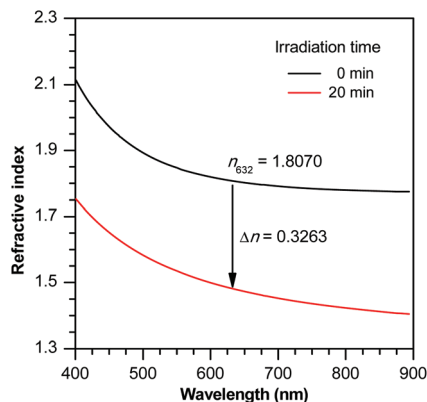


Fig. 6 Wavelength dependence of refractive indices of thin films of P1 before and after UV irradiation.

After exposing its thin film to UV light for 20 min, the RI value drops significantly to 1.7524–1.4044 in the wavelength range of 400–900 nm and decreases by 0.3263 at 632.8 nm.

### Chromatic dispersion

Chromatic dispersion ( $D$ ) describes the optical frequency dependence or variation of the RI of a material with wavelength. Polymers with small  $D$  values are promising for optical applications to reduce chromatic aberration, while those with large  $D$  values may lead to unfavorable effects such as decreased image resolution. The Abbé number ( $\nu_D$ ) is a parameter used to measure the variation or dispersion in RI of a material with wavelength and is defined as  $(n_D - 1)/(n_F - n_C)$ , where  $n_D$ ,  $n_F$  and  $n_C$  are the RI values at Fraunhofer D, F and C lines of 589.2, 486.1 and 656.3 nm, respectively. As shown in Table 6, the  $\nu_D$  values of P1 before and after UV irradiation are 7.4 and 3.9, respectively, and the corresponding  $D$  values (the reciprocal of  $\nu_D$ ) are around 0.135 and 0.259, respectively. The RI values and the Abbé numbers of P1 are quite low compared with many advanced organic materials, indicating that P1 is a potential material for optical applications.

### Photopatterning

Fluorescent photopatterns are in urgent need in a variety of applications such as photonic and electronic devices and biological sensing and probing. Thanks to its good film-forming ability, light-emitting TPE unit and photosensitivity, P1 was utilized to generate a luminescent photopattern by photolithography. The thin film of P1 prepared by solution spin-coating

Table 6 Refractive indices and chromatic dispersions of P1<sup>a</sup>

Irradiation time	$n_{632.8}$	$\nu_D$	$D$
0 min	1.8070	7.4	0.135
20 min	1.4807	3.9	0.259

<sup>a</sup> Abbreviation:  $n$  = refractive index,  $\nu_D$  = Abbé number =  $(n_D - 1)/(n_F - n_C)$ , where  $n_D$ ,  $n_F$  and  $n_C$  are the RI values at wavelengths of 589.2, 486.1 and 656.3 nm, respectively,  $D$  = chromatic dispersion =  $1/\nu_D$ .

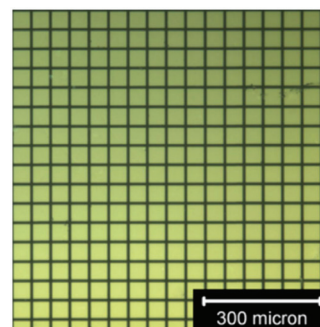


Fig. 7 Fluorescent photopattern generated by UV irradiation of P1. The photograph was taken under UV light illumination (330–385 nm).

was subjected to irradiation with UV light in air for 20 min through a copper photomask. The unexposed region remains emissive (squares), while the fluorescence of the exposed regions was quenched (lines), presumably due to the photo-oxidation reaction. Thus, a fluorescent pattern with high resolution and sharp edges was observed under a fluorescence microscope (Fig. 7).

## Conclusions

In this work, we developed a transition metal-free polymerization route to functional polydiynes from a haloalkyne-based organic reaction. Mediated by an inexpensive additive of KI under nitrogen at 120 °C, the polymerizations of bis(haloalkyne)s proceed well, generating polydiynes in a short period of time in moderate to satisfactory yields. All the polymers are thermally stable with high degradation temperatures. Among the three polymers, only P1 possesses good solubility in common organic solvents. It can form a tough thin film which shows high, UV-tunable refractive indices ( $n = 2.1125$ – $1.7747$ ) in a wide range of wavelengths (400–900 nm). A well-defined fluorescent photopattern of P1 was acquired under UV light through the photolithography process. Thus, the present result provides a facile and straightforward approach for the synthesis of conjugated polymers with extraordinary optical properties and high thermal stability.

## Experimental section

### General information

Diene **4** and monoynone **8** were synthesized according to previously published procedures, while compounds **5** and **6** were prepared by using literature methods.<sup>46,48</sup> All other reagents used for monomer synthesis and polymerization reactions were purchased from Aldrich and used as received without further purification. DMF used for the polymerization was purchased from J&K with molecular sieves in the sealed bottle. Other solvents including DMSO, 1,4-dioxane, *o*-xylene and methanol were purchased from Aldrich.

Weight- ( $M_w$ ) and number-average ( $M_n$ ) molecular weights and polydispersities ( $M_w/M_n$ ) of the polymers were estimated by a Waters gel permeation chromatography (GPC) system equipped with a Waters 515 HPLC pump, a set of Styragel columns (HT3, HT4 and HT6; molecular weight range:  $10^2$  to  $10^7$ ), a column temperature controller, a Waters 486 wavelength-tunable UV-vis detector and a Waters 2414 differential refractometer. The polymers were dissolved in THF ( $\sim 1$  mg mL $^{-1}$ ) and filtered through 0.45  $\mu$ m PTFE syringe-type filters before being injected into the GPC system. THF was used as an eluent at a flow rate of 1.0 mL min $^{-1}$ . The column temperature was maintained at 40 °C and the working wavelength of the UV-vis detector was set at 254 nm. A set of monodisperse polystyrene standards (from Waters) covering the molecular weight range of  $10^3$  to  $10^7$  were used for the molecular weight calibration. The IR spectra were recorded on a Perkin-Elmer 16 PC FTIR spectrophotometer.  $^1$ H and  $^{13}$ C NMR spectra were measured on Bruker ARX 400 NMR spectrometers using DCM- $d_2$  as a solvent. High resolution mass spectra (HRMS) were recorded on a GCT Premier CAB 048 mass spectrometer operated in a MALDI-TOF model. Single crystal X-ray diffraction intensity data were recorded at room temperature on a Bruker-Nonices Smart Apex CCD diffractometer with graphite-monochromated Mo K $_{\alpha}$  radiation. The processing of the intensity data was carried out through the SAINT and SADABS routines and the structure and refinement were obtained by employing the SHELTL suite of X-ray programs (version 6.10). Thermogravimetric analyses (TGA) were conducted under nitrogen on a Perkin-Elmer TGA 7 analyzer at a heating rate of 10 °C min $^{-1}$ . The refractive indices (RI or  $n$ ) were determined on a J A Woollam variable angle ellipsometry system with a wavelength tunability from 400 to 900 nm. Photopatterning of the polymer film was conducted on a Spectroline ENF-280C/F UV lamp at a distance of 3 cm as the light source. The incident light intensity was  $\sim 18.5$  mW cm $^{-2}$ . The films for RI measurement and photopattern were prepared by spin-coating the polymer solution (10 mg of P1 in 1 mL of 1,2-dichloroethane) at 1000 rpm for 1 min on a silicon wafer. The polymer film was dried in a vacuum oven at room temperature overnight. The pattern was generated by UV irradiation of the polymer film through a copper photomask for 20 min. The photograph was taken on an optical microscope (Olympus BX 41) under a UV light source.

### Monomer synthesis

Into a round-bottom flask was dissolved diyne **4** (5.0 mmol, 1.90 g) in methanol (30 mL). The mixture was cooled to 0 °C and 1.40 g (25.0 mmol) of KOH was then added. After stirring at 0 °C for 30 min, NIS (12.5 mmol, 2.81 g) was added. The reaction mixture was further stirred at 0 °C for 15 min. The ice bath was removed and the reaction mixture was stirred at room temperature for another 1 h. The reaction mixture was extracted with DCM and brine 3 times. The organic layer was collected, dried over MgSO $_4$ , filtered and evaporated. The crude product was purified by silica gel column chromatography using hexane/DCM as the eluent to give monomer **1** as

a pale yellow solid (2.88 g, 91%). IR (KBr),  $\nu$  (cm $^{-1}$ ): 3076, 3053, 3026, 2956, 2925, 2853, 2166, 1946, 1914, 1705, 1597, 1495, 1440, 1403, 1383.  $^1$ H NMR (CD $_2$ Cl $_2$ , 400 MHz),  $\delta$  (ppm): 7.21–7.12 (m, 10H), 7.02–6.97 (m, 8H).  $^{13}$ C NMR (CD $_2$ Cl $_2$ , 100 MHz),  $\delta$  (ppm): 144.82, 144.71, 143.47, 143.37, 141.60, 132.23, 132.09, 131.67, 131.65, 128.42, 128.27, 127.42, 127.29, 125.90, 122.04, 121.89, 94.56, 30.64. HRMS (MALDI-TOF):  $m/z$  631.9492 ( $M^+$ , calcd 631.9498).

Monomers **2** and **3** and compound **9** were prepared by the same procedures using compounds **5**, **6** and **8** as starting materials. Below are their characterization data.

**Monomer 2.** IR (KBr),  $\nu$  (cm $^{-1}$ ): 3034, 2160, 1905, 1657, 1501, 1484, 1401, 1363, 1232, 1118, 1102, 1059, 1016.  $^1$ H NMR (CD $_2$ Cl $_2$ , 400 MHz),  $\delta$  (ppm): 7.38 (s, 4H).  $^{13}$ C NMR (CD $_2$ Cl $_2$ , 100 MHz),  $\delta$  (ppm): 132.55, 132.47, 132.28, 124.01, 93.68, 29.50. HRMS (MALDI-TOF):  $m/z$  377.8407 ( $M^+$ , calcd 377.8402).

**Monomer 3.** IR (KBr),  $\nu$  (cm $^{-1}$ ): 3033, 2158, 1694, 1660, 1598, 1552, 1537, 1488, 1393, 1377, 1221, 1108, 1006.  $^1$ H NMR (CD $_2$ Cl $_2$ , 400 MHz),  $\delta$  (ppm): 7.57–7.56 (4H), 7.52–7.50 (4H).  $^{13}$ C NMR (CD $_2$ Cl $_2$ , 100 MHz),  $\delta$  (ppm): 140.72, 133.14, 132.94, 127.25, 127.17, 123.03, 94.02, 30.23. HRMS (MALDI-TOF):  $m/z$  453.8702 ( $M^+$ , calcd 453.8715).

**Compound 9.** IR (KBr),  $\nu$  (cm $^{-1}$ ): 3052, 3021, 2160, 1951, 1598, 1573, 1503, 1489, 1442, 1403, 1181, 1154, 1109, 1072, 1029, 1019.  $^1$ H NMR (CD $_2$ Cl $_2$ , 400 MHz),  $\delta$  (ppm): 7.20–7.18 (2H), 7.16–7.14 (9H), 7.07–7.05 (6H), 7.03–7.01 (2H).  $^{13}$ C NMR (CD $_2$ Cl $_2$ , 100 MHz),  $\delta$  (ppm): 142.27, 140.47, 131.92, 131.58, 131.54, 131.50, 128.16, 128.12, 128.02, 127.07, 126.97, 126.94, 121.45, 94.38, 31.95. HRMS (MALDI-TOF):  $m/z$  482.0529 ( $M^+$ , calcd 482.0531).

### Synthesis of model compound 7

Into a 50 mL Schlenk tube equipped with a stirring bar were added compound **9** (0.8 mmol, 386 mg) and KI (1.6 mmol, 265 mg). The Schlenk tube was then vacuum purged with nitrogen 3 times. DMF (5 mL) was injected into the tube using a hypodermic syringe. The resulting mixture was stirred at 120 °C for 6 h in a nitrogen environment. The reaction mixture was then cooled to room temperature, extracted with DCM and washed with brine 3 times. The organic layer was collected, dried over MgSO $_4$ , filtered and evaporated. The crude product was purified using silica gel column chromatography using the hexane/DCM mixture as the eluent to give model compound **7** as a yellow solid (150 mg, 53%). IR (KBr),  $\nu$  (cm $^{-1}$ ): 3074, 3053, 3025, 2923, 2853, 2196, 2146, 1949, 1630, 1598, 1491, 1443, 1403.  $^1$ H NMR (CD $_2$ Cl $_2$ , 400 MHz),  $\delta$  (ppm): 7.30 (d, 4H), 7.19–7.14 (m, 18H), 7.07–7.03 (m, 16H).  $^{13}$ C NMR (CD $_2$ Cl $_2$ , 100 MHz),  $\delta$  (ppm): 145.13, 143.43, 143.30, 143.18, 142.12, 140.08, 131.74, 131.37, 131.23, 131.15, 131.12, 127.83, 127.76, 127.64, 126.77, 126.63, 126.61, 119.34, 81.75, 73.92. HRMS (MALDI-TOF):  $m/z$  710.2954 ( $M^+$ , calcd 710.2974).

### Polymerization

All the polymerization reactions were carried out under a nitrogen flow in a Schlenk tube. A typical procedure for the polymerization of **1** under optimized conditions is given below

as an example (Table 2, no. 3). In a 10 mL Schlenk tube with a two-way stopcock on the sidearm were charged **1** (0.2 mmol, 126.4 mg) and KI (0.4 mmol, 66.4 mg) under nitrogen. After vacuum and purging with nitrogen for 3 cycles, 2 mL of DMF was injected into the tube using a hypodermic syringe. The resulting mixture was stirred at 120 °C for 6 h under a nitrogen flow. Afterwards, the solution was added dropwise into 100 mL of methanol *via* a cotton filter under stirring. The precipitate was collected by centrifugation, washed with hexane and dried under vacuum at room temperature to a constant weight. A brownish yellow powder of polymer P1 was obtained in 72% yield.  $M_w$  20 100;  $M_w/M_n$  2.4. IR (KBr),  $\nu$  ( $\text{cm}^{-1}$ ): 3077, 3053, 3025, 2959, 2923, 2191, 2142, 1946, 1911, 1641, 1598, 1492, 1441, 1403, 1384.  $^1\text{H}$  NMR ( $\text{CD}_2\text{Cl}_2$ , 400 MHz),  $\delta$  (ppm): 7.26, 7.12, 7.01, 3.10.  $^{13}\text{C}$  NMR ( $\text{CD}_2\text{Cl}_2$ , 100 MHz),  $\delta$  (ppm): 145.19, 145.03, 143.30, 143.14, 141.60, 132.38, 132.19, 131.77, 131.64, 128.40, 128.21, 127.45, 127.27, 120.22, 120.02, 83.81, 82.19, 77.86, 74.63.

P2: yield 53%. No characterization could be done due to the insolubility of the polymer.

P3: yield 44%. No characterization was done as the polymer was insoluble.

## Acknowledgements

This work was partially supported by the National Basic Research Program of China (973 Program; 2013CB834701 and 2013CB834702), the University Grants Committee of Hong Kong (AoE/P-03/08), the National Science Foundation of China (21490570 and 21490574), the Research Grants Council of Hong Kong (604913, 16303815 and 16305014) and the Innovation and Technology Commission (ITC-CNRC14SC01). B.Z.T. acknowledges the support from the Guangdong Innovative Research Team Program (201101C0105067115).

## References

- 1 A. J. Heeger, *Synth. Met.*, 2001, **125**, 23–42.
- 2 A. G. MacDiarmid, *Synth. Met.*, 2001, **125**, 11–22.
- 3 M. B. Nielsen and F. Diederich, *Chem. Rev.*, 2005, **105**, 1837–1867.
- 4 V. D. Bock, H. Hiemstra and J. H. van Maarseveen, *Eur. J. Org. Chem.*, 2006, 51–68.
- 5 T. Aokia, T. Kanekoa and M. Teraguchi, *Polymer*, 2006, **47**, 4867–4892.
- 6 W. H. Binder and R. Sachsenhofer, *Macromol. Rapid Commun.*, 2007, **28**, 15–54.
- 7 Y. Morisaki and Y. Chujo, *Prog. Polym. Sci.*, 2008, **33**, 346–364.
- 8 M. Shiotsuki, F. Sanda and T. Masuda, *Polym. Chem.*, 2011, **2**, 1044–1058.
- 9 A. Yoshimura, A. Nomoto and A. Ogawa, *Res. Chem. Intermed.*, 2014, **40**, 2381–2389.
- 10 J. R. Castanon, N. Sano, M. Shiotsuki and F. Sanda, *ACS Macro Lett.*, 2014, **3**, 51–54.
- 11 Y. Miyagi, H. Sogawa, M. Shiotsuki and F. Sanda, *Macromolecules*, 2014, **47**, 1594–1603.
- 12 J. W. Y. Lam, Y. P. Dong, K. K. L. Cheuk, J. D. Luo, Z. L. Xie, H. S. Kwok, Z. S. Mo and B. Z. Tang, *Macromolecules*, 2002, **35**, 1229–1240.
- 13 J. W. Y. Lam and B. Z. Tang, *Acc. Chem. Res.*, 2005, **38**, 745–754.
- 14 J. Liu, J. W. Y. Lam and B. Z. Tang, *Chem. Rev.*, 2009, **109**, 5799–5867.
- 15 A. Qin, J. W. Lam and B. Z. Tang, *Chem. Soc. Rev.*, 2010, **39**, 2522–2544.
- 16 A. Qin, J. W. Y. Lam and B. Z. Tang, *Prog. Polym. Sci.*, 2012, **37**, 182–209.
- 17 R. Hu, N. L. Leung and B. Z. Tang, *Chem. Soc. Rev.*, 2014, **43**, 4494–4562.
- 18 Z. Li, A. J. Qin, J. W. Y. Lam, Y. P. Dong, Y. Q. Dong, C. Ye, I. D. Williams and B. Z. Tang, *Macromolecules*, 2006, **39**, 1436–1442.
- 19 J. B. Shi, C. J. W. Jim, F. Mahtab, J. Z. Liu, J. W. Y. Lam, H. H. Y. Sung, I. D. Williams, Y. P. Dong and B. Z. Tang, *Macromolecules*, 2010, **43**, 680–690.
- 20 R. H. Zheng, M. Haussler, H. C. Dong, J. W. Y. Lam and B. Z. Tang, *Macromolecules*, 2006, **39**, 7973–7984.
- 21 M. Haussler, J. Z. Liu, R. H. Zheng, J. Wing, Y. Lam, A. J. Qin and B. Z. Tang, *Macromolecules*, 2007, **40**, 1914–1925.
- 22 J. Z. Liu, R. H. Zheng, Y. H. Tang, M. Haussler, J. W. Y. Lam, A. Qin, M. X. Ye, Y. N. Hong, P. Gao and B. Z. Tang, *Macromolecules*, 2007, **40**, 7473–7486.
- 23 C. Y. K. Chan, J. W. Y. Lam, C. K. W. Jim, H. H. Y. Sung, I. D. Williams and B. Z. Tang, *Macromolecules*, 2013, **46**, 9494–9506.
- 24 H. K. Li, J. Z. Sun, A. J. Qin and B. Z. Tang, *Chin. J. Polym. Sci.*, 2012, **30**, 1–15.
- 25 A. J. Qin, J. W. Y. Lam, C. K. W. Jim, L. Zhang, J. J. Yan, M. Haussler, J. Z. Liu, Y. Q. Dong, D. H. Liang, E. Q. Chen, G. C. Jia and B. Z. Tang, *Macromolecules*, 2008, **41**, 3808–3822.
- 26 A. J. Qin, J. W. Y. Lam, L. Tang, C. K. W. Jim, H. Zhao, J. Z. Sun and B. Z. Tang, *Macromolecules*, 2009, **42**, 1421–1424.
- 27 Y. Liu, J. Wang, D. Huang, J. Zhang, S. Guo, R. Hu, Z. Zhao, A. Qin and B. Z. Tang, *Polym. Chem.*, 2015, **6**, 5545–5549.
- 28 H. K. Li, J. Mei, J. A. Wang, S. A. Zhang, Q. L. Zhao, Q. A. Wei, A. J. Qin, J. Z. Sun and B. Z. Tang, *Sci. China: Chem.*, 2011, **54**, 611–616.
- 29 H. K. Li, J. Wang, J. Z. Sun, R. R. Hu, A. J. Qin and B. Z. Tang, *Polym. Chem.*, 2012, **3**, 1075–1083.
- 30 H. K. Li, Z. Wang, J. Li, E. G. Zhao, J. Z. Sun, J. W. Y. Lam, A. J. Qin and B. Z. Tang, *Macromol. Chem. Phys.*, 2014, **215**, 1036–1041.
- 31 B. C. Yao, J. Z. Sun, A. J. Qin and B. Z. Tang, *Chin. Sci. Bull.*, 2013, **58**, 2711–2718.
- 32 J. Z. Liu, J. W. Y. Lam, C. K. W. Jim, J. C. Y. Ng, J. B. Shi, H. M. Su, K. F. Yeung, Y. N. Hong, M. Faisal, Y. Yu, K. S. Wong and B. Z. Tang, *Macromolecules*, 2011, **44**, 68–79.
- 33 C. K. W. Jim, A. Qin, J. W. Y. Lam, F. Mahtab, Y. Yu and B. Z. Tang, *Adv. Funct. Mater.*, 2010, **20**, 1319–1328.



- 34 B. C. Yao, J. Mei, J. Li, J. Wang, H. Q. Wu, J. Z. Sun, A. J. Qin and B. Z. Tang, *Macromolecules*, 2014, **47**, 1325–1333.
- 35 A. S. Abd-El-Aziz, *Macromol. Rapid Commun.*, 2002, **23**, 995–1031.
- 36 F. Hide, M. A. DiazGarcia, B. J. Schwartz and A. J. Heeger, *Acc. Chem. Res.*, 1997, **30**, 430–436.
- 37 C. K. W. Jim, J. W. Y. Lam, A. J. Qin, Z. J. Zhao, J. Z. Liu, Y. N. Hong and B. Z. Tang, *Macromol. Rapid Commun.*, 2012, **33**, 568–572.
- 38 F. Diederich, P. J. Stang and R. R. Tykwinski, *Acetylene Chemistry: Chemistry, Biology and Material Science*, Wiley-VCH, Weinheim, Germany, 2005.
- 39 J. M. Lehn, *Supramolecular Chemistry: Concepts and Perspectives*, VCH, Weinheim, Germany, 1995.
- 40 C. Glaser, *Ber. Dtsch. Chem. Ges.*, 1869, **2**, 422–424.
- 41 A. Hay, *J. Org. Chem.*, 1960, **25**, 1275–1276.
- 42 R. R. Hu, R. Q. Ye, J. W. Y. Lam, M. Li, C. W. T. Leung and B. Z. Tang, *Chem. – Asian J.*, 2013, **8**, 2436–2445.
- 43 M. Häussler, R. Zheng, J. W. Lam, H. Tong, H. Dong and B. Z. Tang, *J. Phys. Chem. B*, 2004, **108**, 10645–10650.
- 44 W. Q. Wu and H. F. Jiang, *Acc. Chem. Res.*, 2014, **47**, 2483–2504.
- 45 Z. Chen, H. Jiang, A. Wang and S. Yang, *J. Org. Chem.*, 2010, **75**, 6700–6703.
- 46 R. Hu, J. W. Y. Lam, J. Liu, H. H. Y. Sung, I. D. Williams, Z. Yue, K. S. Wong, M. M. F. Yuen; and B. Z. Tang, *Polym. Chem.*, 2012, **3**, 1481–1489.
- 47 M. V. Russo, C. L. Sterzo, P. Franceschini, G. Biagini; and A. Furlani, *J. Organomet. Chem.*, 2001, **619**, 49–61.
- 48 H. Peng, L. Cheng, J. Luo, K. Xu, Q. Sun, Y. Dong, F. Salhi, P. P. S. Lee, J. Chen and B. Z. Tang, *Macromolecules*, 2002, **35**, 5349–5351.